International Journal of Refrigeration 165 (2024) 45–57

Contents lists available at ScienceDirect

International Journal of Refrigeration

journal homepage: www.elsevier.com/locate/ijrefrig

High-glide refrigerant blends in high-temperature heat pumps: Part 2 – Inline composition determination for binary mixtures

Mélanges de frigorigènes à haut glissement de température dans les pompes à chaleur à haute température : Partie 2 – Détermination en ligne de la composition des mélanges binaires

Leon P.M. Brendel [a,*], Silvan N. Bernal [a], Carl Hemprich [b], Aaron J. Rowane [c], Ian H. Bell [c], Dennis Roskosch [b], Cordin Arpagaus [a], André Bardow [b], Stefan S. Bertsch [a]

[a] Institute for Energy Systems, Eastern Switzerland University of Applied Sciences, 9471 Buchs, Switzerland
[b] Energy and Process Systems Engineering, ETH Zürich, 8092 Zürich, Switzerland
[c] National Institute of Standards and Technology, Material Measurement Laboratory, Applied Chemicals and Materials Division, Boulder, CO 80305-3337, United States

ARTICLE INFO

Keywords:
High-temperature heat pump
Composition determination
Refrigerants
Blends
Mixtures
Inline
Online

Mots clés:
Pompe à chaleur à haute température
Détermination de la composition
Frigorigènes
Mélanges
En ligne

ABSTRACT

Refrigerant mixtures are frequently used in air-conditioners and heat pumps. However, mixtures with high glides of 30 K and more during evaporation are rare, partially because there is an increased concern about composition shifts within the system. An easy and reliable inline composition measurement could alleviate these concerns and simplify the handling of systems with high-glide mixtures. This study investigates six composition determination methods, which are all non-invasive, five of which can be conducted during system operation. All methods were applied to all available mixtures in a dataset of 380 data points. The binary and ternary mixtures tested consist of the refrigerants R-1233zd(E), R-1336mzz(Z), R-1234yf, R-1224yd(Z), and R-32. Each method was applied to all datapoints collected with a certain refrigerant mixture at varying operating conditions. The average of the calculated mass fraction was then compared to the manually charged mass fraction. For the density method, this difference of the calculated and measured mass fraction was always less than 0.03 and usually smaller than 0.01 across all tested mixtures. Most other methods performed well with deviations typically less than 0.05. Some of the methods require only low-cost sensors like thermocouples and pressure transducers. Property data of ternary mixtures is also discussed in the study but a composition determination, theoretically possible combining any two of the six methods, is not attempted in this study.

1. Introduction

Refrigerant mixtures are very common in various applications. Frequently, a refrigerant that is phased out must be replaced with a refrigerant blend, approximating certain properties while satisfying requirements for global warming potential or flammability. In most cases, a resulting temperature glide during evaporation and condensation is an undesired byproduct rather than a desired feature. Therefore, the mixtures are usually designed for a low glide. However, for industrial heat pumps, certain applications can greatly benefit from a large glide, as experimentally shown in Brendel et al. (2023). This benefit motivates research on mixtures with glides of 25 K and more. More context is given in Part 1 of this study.

However, the higher the glide, the higher are concerns about the practicability of the mixtures:

- If leakage occurs, the mixture components will usually leak at different rates, shifting the composition.
- Different oil solubility could shift the circulating composition.
- Liquid hold-up or not well mixed volumes of liquid could change the composition.

For the above reasons, an inexpensive and reliable composition measurement would be highly beneficial. Presently, gas

* Corresponding author.
E-mail address: leon.brendel@ost.ch (L.P.M. Brendel).

https://doi.org/10.1016/j.ijrefrig.2024.05.012
Received 17 January 2024; Received in revised form 21 March 2024; Accepted 5 May 2024
Available online 10 May 2024

chromatography (GC) is the most common composition measurement but has distinct disadvantages including its high-cost, invasive sampling, and time consuming analysis. The advantages of GC include high accuracy and it provides a direct measurement of the composition. However, several lower-cost, non-invasive techniques have been proposed in the literature. These techniques involve either measuring fluid properties or cycle performance and back calculating the composition using a reliable equation of state (EoS). Table 1 lists studies conducting composition measurements and gives basic information for each. Looking at the various studies points to several gaps in the literature regarding composition determination:

Table 1
Overview of experimental research on composition determination of refrigerant mixtures.

Name and year	Refrigerant mixture(s) and property model	Approach of composition determination	Comments
Chen and Kruse (1995)	R-23/152a, Carnahan-Starling-DeSantis EOS	Differential hold-up model for evaporator and condenser	
Sumida et al. (1998)	R-407C, REFPROP	Evaporator inlet temperature + empirical leakage correlation	
Johansson and Lundqvist (2001)	R-407C, REFPROP	Evaporator inlet temperature + empirical leakage correlation	
Fukuta et al. (2006)	Refrigerants: R-410A, R-134a, R-600a Refrigeration oils: PVE for R-410A, PAG for R-134a, paraffinic mineral oil for R-600a	Refractive index	Determined the composition of refrigerant–oil mixtures. The study also shows successful transient measurements.
Aprea et al. (2009)	R-407C, REFPROP	Evaporator inlet temperature + empirical leakage correlation	With similarities to Johansson and Lundqvist, 2001
Fukuda et al. (2012)	R-32/1234ze(E)	Gas chromatography	
Bao et al. (2016)	Pentane/ Isobutane, REFPROP	Density	
Zhang et al. (2021)	R-134a/245fa, REFPROP	Density	The study also proposes to measure the enthalpy change between the inlet of the preheater and the outlet of the evaporator to determine mixture composition.
Chen et al. (2021)	R-290/600a	Gas chromatography	Measured linear relationships between circulating and charged concentration.
Quenel et al. (Quenel et al., 2023)	Propane/ Isobutene, REFPROP	Evaporator inlet temperature	Similar method to Sumida et al., 1998 and Johansson and Lundqvist, 2001, but without empirical leakage correlation (not needed because only investigate binary mixtures, not a ternary mixture).
Miyawaki et al. (2023)	R-32/1234yf	NIR Absorption Spectroscopy	

- A comparison of different methods on one dataset would provide best direct comparability but is missing
- Datasets with a large number of different mixtures do not exist.
- Several other methods are theoretically suitable for composition determination but have not been verified experimentally.

Online composition determination can be realized from any measured quantity that is sensitive to mixture composition. This involves minimizing the difference between the measured property and a value calculated with an EOS using the mass fraction as an iteration variable. As an introductory example, Fig. 1 shows how a density measurement can be used in conjunction with an EoS to determine the composition of a binary mixture. The density of a R-32/1224yd(Z) mixture was measured using a Coriolis-type densimeter during heat pump operation at a temperature of 65.8 °C and a pressure of 2482.9 kPa. The measured density was 1128.5 kg/m^3. The composition of the mixture was calculated using a mixture model implemented in REFPROP v10.0 (Lemmon et al., 2018) where the measured temperature, pressure and density were inputs. The black line is the calculated density of the mixture at a fixed temperature and pressure as a function of the R-1224yd(Z) mass fraction. The inset plot shows a zoom of the area of the intersection. At the charged mass fraction of 0.83, the predicted density is 1116.5 kg/m^3. The mass fraction at the measured density is approximately 0.846. Hence, there is a 1.1% deviation between the measured and expected density and a deviation of 0.016 between the expected and calculated mass fraction. This deviation of measured and calculated density is not surprising given the accuracy of the sensors (±10 kg m^{-3} for density, ±75 kPa for pressure, ±1.5 K for temperature, according to the manufacturers rating). Additionally, the REFPROP prediction has an uncertainty, the charging procedure has an uncertainty, and the pressure and temperature sensors are not directly at the density meter, further introducing small errors. Lastly, a composition shift could have occurred from different oil-solubilities or liquid hold-up. Cumulatively, these impacts can easily explain the 1.1% deviation. The positive outcome is, that despite the various uncertainty contributions, the calculated and charged mass fraction deviated by only 0.016. It is important to note that with a single thermophysical property the composition determination can only be readily applied for binary mixtures, while composition determination of a ternary mixture would require two property measurements.

This approach is also visualized in Fig. 2. One can combine information A and B to calculate the properties measured in D and make a comparison (C). Alternatively, The measurements in A and D can be assumed to be correct in order to calculate the mass fraction of a mixture in B. This results in numerous possible methods of composition

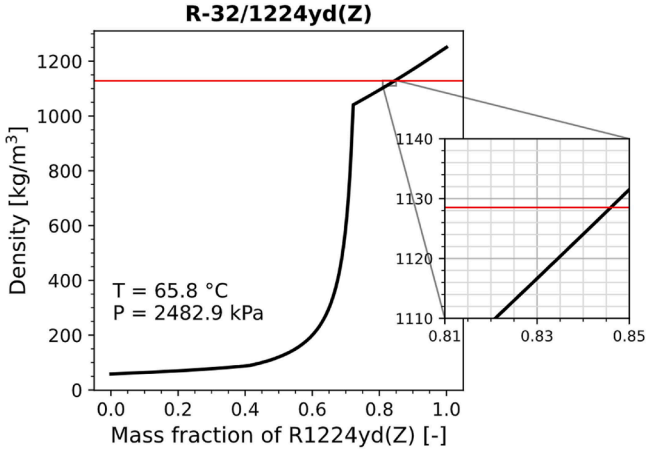

Fig. 1. Density curve as a function of mixture composition at fixed temperature and pressure calculated from REFPROP overlaid with measured density in the liquid line and charged mass fraction.

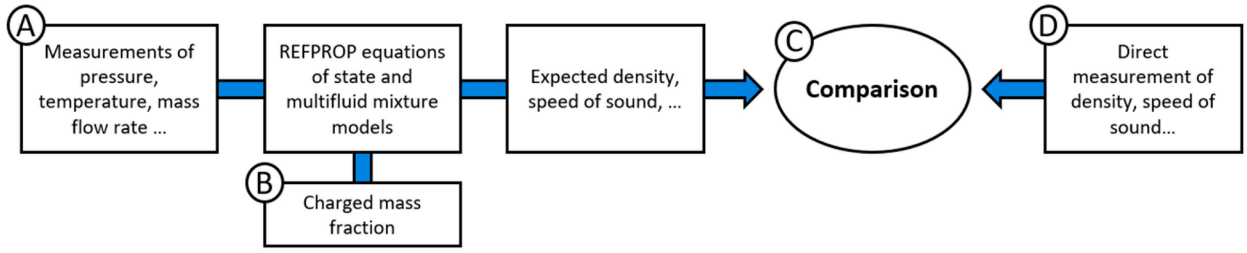

Fig. 2. Comparison of measurements with mixture equations implemented in REFPROP v10.

determination using different measurements. Inevitably, experimental investigations are needed to find the combined effect of multiple error sources, such as poor mixture models, refrigerant losses during charging, different oil solubility of refrigerants, and measurement uncertainty of various sensors.

In this study six different composition determination methods were applied on a large dataset of mixtures at varying compositions. The measurements of the six methods and, therefore, the names of the methods are as follows:

1. Evaporator Inlet Temperature
2. Dew Point Temperature
3. Density
4. Speed of Sound
5. Condenser Energy balance
6. Resting Pressure

The methods will be more thoroughly explained in the paper and their accuracy is discussed based on approximately 380 experimental datapoints.

2. Methodology

2.1. Experimental test setup

Tests were conducted on a laboratory-scale high-temperature heat pump (HTHP) with an approximate heating capacity of 10 kW, featuring optional use of an internal heat exchanger. A reciprocating compressor was used with RenisoTriton SE170 as a high-viscosity and high-temperature oil (Fuchs, 2023, 2022). The evaporator, condenser, and internal heat exchanger were of type flat plate and used in counterflow configuration. Other components were an oil separator, a receiver, and a suction line accumulator. While the oil separator is important for some of the proposed methods, the receiver and accumulator were installed for the system and compressor level tests. A more detailed description and schematic, including these components, can be found in Part 1 of this paper (Brendel et al., 2024).

One sight glass was installed upstream of the expansion valve and another one downstream of the evaporator, both in a horizontal orientation. A Coriolis type mass flow meter that can also measure density, and a speed of sound sensor, were installed in the liquid line upstream of the expansion valve close to the first sight glass. The heat source and sink were water. The heat sink flow rate was measured using a Coriolis mass flow meter. Fig. 3 is a schematic showing the most important components and the measurement location for the six methods, as discussed in the next section.

2.2. Tested pure refrigerants and mixtures

Table 2 provides information on the pure fluids, binary, and ternary mixtures tested in this study. The column headers have the following meaning:

- Letter: Unique identifier for one set of data points tested without changing the charge of any mixture component. The letter changes even if a mixture or pure fluid is tested again. The letter also shows the chronological order of the tests, with the only exception being K2, which was tested between the O and P series. The letters "I" and "U" were omitted.
- Mixture components and compositions
  - Refrigerants 1, 2 and 3: Refrigerants in the mixture.
  - Charge: Total mass of charged refrigerant.
  - x_1, x_2, x_3: Charged mass fractions (mass fractions according to measured weight of refrigerant during charging)
- Operating conditions
  - P_{low}: Range of low side pressures tested
  - P_{high}: Range of high side pressures tested
- Number of datapoints
  - Total: Number of data points
  - with IHX: Number of data points with activated IHX

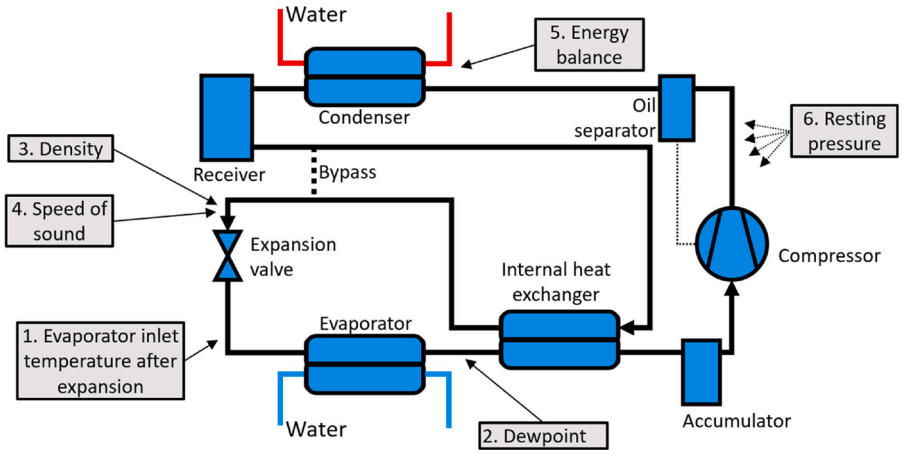

Fig. 3. Schematic of the HTHP with an indication of measurement locations for the six composition determination methods.

Table 2
Tested mixtures and compositions as well as pure fluids.

Letter*	Type	Mixture components			Charge and composition				Operating conditions		Number of data points					
		Refrigerant 1	Refrigerant 2	Refrigerant 3	Charge [g]	x_1	x_2	x_3	P_{low} [kPa]	P_{high} [kPa]	Total	with IXH	w/o IHX	DP	RP	disk.
A	Pure	R-1233zd(E)			4500				52–481	200–2544	26	5	15	5	1	3
E	Pure	R-1336mzz(Z)			4500				48–357	315–1745	31	9	18	3	1	0
H	Pure	R-1234yf			4500				164–984	1149–3168	23	7	13	2	1	8
K	Pure	R-1224yd(Z)			4502				111–384	880–2389	21	9	8	3	1	0
K2	Pure	R-1224yd(Z)			4000				147–258	833–1725	19	12	7	0	0	2
B	Binary	R-1233zd(E)	R-1234yf		5293	0.85	0.15		52–486	482–2609	38	8	25	4	1	8
C	Binary	R-1233zd(E)	R-1234yf		4500	0.7	0.3		104–524	813–2659	29	18	8	3	0	9
D	Binary	R-1233zd(E)	R-1234yf		5727	0.55	0.45		106–602	683–2719	22	7	10	4	1	5
F	Binary	R-1336mzz(Z)	R-1234yf		5000	0.9	0.1		77–437	479–2059	21	10	7	3	1	13
G	Binary	R-1336mzz(Z)	R-1234yf		6000	0.75	0.25		110–546	700–2037	16	11	2	3	0	10
AA	Binary	R-1336mzz(Z)	R-1234yf		3714	0.65	0.35		209–250	1200–1324	4	2	0	1	1	0
AB	Binary	R-1336mzz(Z)	R-1234yf		4010	0.6	0.4		228–270	1286–1419	2	2	0	0	0	0
AC	Binary	R-1336mzz(Z)	R-1234yf		4375	0.55	0.45		251–295	1398–1548	4	2	0	1	1	0
J	Binary	R-1336mzz(Z)	R-1234yf		6000	0.2	0.8		158–809	738–2797	22	10	8	3	1	5
P	Binary	R-1224yd(Z)	R-32		4040	0.99	0.01		157–217	1057–1114	2	2	0	0	0	0
Q	Binary	R-1224yd(Z)	R-32		4124	0.97	0.03		185–245	1150–1231	3	2	0	0	1	0
L	Binary	R-1224yd(Z)	R-32		4739	0.95	0.05		213–293	1245–1381	9	5	0	3	1	2
M	Binary	R-1224yd(Z)	R-32		5002	0.9	0.1		259–352	1628–1867	6	4	0	2	0	1
N	Binary	R-1224yd(Z)	R-32		5424	0.83	0.17		153–584	1717–3122	14	7	4	2	1	5
O	Ternary	R-1224yd(Z)	R-32	R-1336mzz(Z)	6029	0.75	0.15	0.1	190–536	1502–2980	8	5	0	2	1	1
R	Ternary	R-1224yd(Z)	R-32	R-1234yf	4341	0.92	0.03	0.05	206–259	1227–1307	2	2	0	0	0	0
S	Ternary	R-1224yd(Z)	R-32	R-1234yf	4593	0.87	0.03	0.1	223–452	1305–1778	13	8	0	3	2	2
T	Ternary	R-1224yd(Z)	R-32	R-1234yf	4851	0.82	0.03	0.15	240–348	1361–1649	4	3	0	0	1	0
V	Ternary	R-1224yd(Z)	R-32	R-1234yf	5155	0.78	0.02	0.2	256–308	1448–1566	2	2	0	0	0	0
W	Ternary	R-1224yd(Z)	R-32	R-1234yf	5498	0.73	0.02	0.25	272–327	1534–2064	8	2	3	1	2	2
X	Ternary	R-1224yd(Z)	R-32	R-1234yf	5540	0.72	0.03	0.25	278–293	1561–1583	3	3	0	0	0	0
Y	Ternary	R-1224yd(Z)	R-32	R-1234yf	5599	0.71	0.04	0.25	287–295	1639–1661	4	2	0	1	1	0
Z	Ternary	R-1224yd(Z)	R-32	R-1234yf	5718	0.7	0.06	0.24	312–614	1805–2548	9	6	0	2	1	0
AD	Ternary	R-1336mzz(Z)	R-1234yf	R-32	4464	0.54	0.44	0.02	267–310	1531–1692	3	2	0	1	0	0
AE	Ternary	R-1336mzz(Z)	R-1234yf	R-32	4605	0.52	0.43	0.05	197–591	1291–2655	12	7	0	3	2	0
All		*R-1336mzz(Z), R-1233zd(E), R-1224yd(Z), R-1234yf, R-32 and mixtures*							*48–984*	*200–3168*	*380*	*174*	*128*	*55*	*23*	*76*

* Letters in chronological order. Rows shaded in gray indicate and separate refrigerant mixtures with the same components but different composition.

- w/o IHX: Number of tests with deactivated IHX
- DP: Number of dew point measurements
- RP: Number of resting pressure measurements.
- disk.: Number of discarded data points, for example, because a lack of subcooling at the expansion valve inlet (undercharged condition).

Mixtures were prepared by subsequently charging each refrigerant and tracking the charged mass of each component with a scale. Refrigerant hoses were filled with refrigerant before starting the charging procedure and not emptied in the charging procedure to minimize losses.

2.3. Computation of mixture composition

Composition determination using a density measurement was already explained in the introduction with Fig. 1 and Fig. 2. If pressure, temperature, the components and the composition of a refrigerant mixture is known, the density can be calculated using REFPROP. On the other hand, if the composition is unknown and the density is known, then the composition can be calculated. It is an equation system that can be solved as long as only one information is missing. The other methods rely on the same idea but use other measured and calculated properties. Each method involves accessing a reference property that can be obtained via a primary and a secondary path. The secondary path invariably entails computing at least one thermophysical property of the mixture, necessitating the mixture components and mass fraction as inputs. E.g., in the introductory example, the density was measured directly (primary path) but also calculated using temperature, pressure and the mass fractions (secondary path). In Fig. 2, D-C would be the primary path while A-C (using B) would be the secondary path). If the reference property values through the primary and secondary path are closely aligned, it suggests either both the measurement and the prediction are flawed and fortuitously coincide, or they verify each other as correct. Instead of performing the comparison, all measurements could be assumed to be correct and the compositions could be deemed unknown. Subsequently, there exists a mass fraction that would yield alignment of the reference property values calculated using the primary and secondary path, which can be found iteratively. For this paper, a primary and secondary path was compared and used for composition determination for six different methods.

Table 3 shows the needed measurements and assumptions for each method presented in this paper. Additionally, important measurements (other than Pressure and Temperature) are listed. The symbols in the equations are introduced as follows: T – temperature, P – pressure, x – mass fraction, q – vapor quality, $\dot{m}$ – mass flow rate, $\dot{Q}$ – heat transfer rate, V – total volume. The subscripts in the equations are introduced as follows: in – inlet, out – outlet, v – valve, e – evaporator (refrigerant side), c – condenser (refrigerant side), si – condenser (water side), equ – equilibrium, hp – heat pump, ref – refrigerant, 1 – component one. The primary and secondary path for each method are shown in the Appendix in Table 8.

The brentq solver from the Python package Scipy (Virtanen et al., 2020) was used for all methods except 'evaporator inlet temperature' to iteratively solve for the mixture composition resulting in the measured property. The bounds were set to 0 and 1, an initial guess value was not provided. For the Evaporator Inlet Temperature method, the least_squares solver from the same Python package was used. The bounds were set to 0 and 1 and the guess value was 0.5.

2.4. Measurement procedures and exclusion of data points

2.4.1. Evaporator inlet temperature, density, speed of sound, energy balance

These four methods require steady-state data. Steady-state was defined by a maximum change over 10 minutes of:

- 1.5 K for the subcooling at the expansion valve inlet
- 5 kPa for the suction pressure
- 15 kPa for the discharge pressure
- 2.5% for the COP

Typically, the changes were much less (compare with Part 1 of this study). Data was collected every second and averaged over 10 min. Datapoints were excluded if there was no subcooling at the expansion valve inlet (undercharged condition). For the Condenser Energy Balance method, data points were removed if the calculated subcooling was less than 0.1 K (measured condenser outlet temperature must be lower than the bubble point temperature) or if the measured condenser inlet temperature was within 0.1 K of the dew point temperature (lack of condenser inlet superheat). Additionally, for the condenser energy balance, data points for which the water temperature changed by less than 3 K were excluded since the 1.5 K thermocouple uncertainty results in a high relative uncertainty of the measured heat transfer rate.

The time needed to reach a steady-state varied from 30 to 120 min as a function of the operating conditions. No correlation was noted as a function of the mixtures or temperature glides. With a charge of approximately 5 kg and flow rates on the order of 2 to 5 kg per minute, the entire charge circulated every 1 to 3 min.

2.4.2. Dew point

For the dew point measurement, the expansion valve was controlled manually. The procedure started from some steady-state. The expansion valve was opened in small increments while observing the sight glass at the evaporator outlet. The valve was opened until the liquid became visible in the form of periodically appearing and disappearing mist or a slow stratified flow, which depended on the flow velocity. These initial occurrences of liquid were used as indicators of a state very close to the dewpoint temperature. When such a flow regime was visible, data was collected for approximately 10 s and averaged in post-processing. The pressure and temperature at the evaporator outlet were then taken as the dewpoint measurement. The Dew Point method is prone to errors since it is a non-equilibrium measurement and requires manual operation. However, the positive results suggest that this method can be useful.

Table 3
Overview of composition determination methods with a list of needed measurements and special sensor where applicable.

Method	Needed measurements and assumptions	Measurements other than T and P	Can apply during operation	Requires sampling
Evaporator inlet temperature	$x_1 = f(P_{v,out}, T_{v,out}, P_{v,in}, T_{v,in})$ Assume: $h_{v,in} = h_{v,out}$ and $h_{v,out} \leq h(P_{v,in}, q = 0)$	None	Yes	No
Dewpoint	$x_1 = f(P_{e,out}, T_{dew}, q = 1)$	Visual inspection	Yes	No
Density	$x_1 = f(P_{v,in}, T_{v,in}, \rho_{v,in})$	Density	Yes	No
Speed of sound	$x_1 = f(P_{v,in}, T_{v,in}, u_{v,in})$	Speed of sound	Yes	No
Energy balance	$x_1 = f(P_{c,in}, T_{c,in}, P_{c,out}, T_{c,out}, \dot{m}_r, T_{si,in}, T_{si,out}, \dot{m}_{si})$ Assume: $\dot{Q}_{c,r} = \dot{Q}_{c,w}$	Water and refrigerant mass flow rate	Yes	No
Resting pressure	$x_1 = (T_{equ}, P_{equ}, V_{hp}, m_r)$	Inner volume of heat pump and total charge	No	No

2.4.3. Resting pressure

Resting pressure measurements were taken in the morning before starting the system. The expansion valve had remained open over night for approximately 10 h. The entire system had time to come to mechanical and thermal equilibrium. Like the dew point measurements, data were taken over 10 s. The resting pressure was defined as the average of six pressure transducers, typically within a range of ±5 kPa. The resting temperature was defined as the average of seven thermocouples, typically within a range of ±1 °C. The inner volume of the heat pump had been measured once by charging 50 g of R-1336mzz(Z) into the system. This resulted in a pressure of 23 kPa at 20.8 °C. Multiplying the charge with the specific volume, the total inner volume was determined to be 32 liters.

2.5. Sensor locations and measurement accuracy

Each method uses data from different sensors. Table 4 explains the sensor locations. Table 5 lists the uncertainties associated with the various measurements.

The propagated uncertainty is strongly dependent on the specific components, mixture composition and operating condition. For the majority of points, the uncertainty was below a range of ±0.05 mass fraction for all methods. Singular outliers exist with propagated uncertainties of 0.2. This was calculated using the uncertainties shown in Table 5 for the respective sensors. Only the uncertainty of the speed of sound sensor was increased to 1 m/s to make a more conservative assumption. An uncertainty of the equations of state and mixture coefficients was not considered.

2.6. REFPROP mixture models

The mixture models in NIST REFPROP version 10.0 operate based on binary mixture interactions. Therefore, for the 5 pure components considered here, there are $5 \times 4/2 = 10$ binary pairs. Of the 10 binary pairs, only one is based upon fitting of experimental data, that of R-32/1234yf (Akasaka, 2013). Since then a newer model has been developed for this binary pair based on publicly available experimental data (Bell, 2023), but it is not yet available in any public release of NIST REFPROP. The remaining 9 binary pairs are all covered by estimation schemes in NIST REFPROP. The review of Bell et al. (2021) found no experimental data for any binary pair studied here aside from R-32/1234yf. Since that publication, one dataset has been published for R-1234yf/1233zd(E), for which the vapor pressures of this mixture are predicted within 2% (Abbadi et al., 2022).

For R-32, the equation of state (EOS) from Tillner-Roth and Yokozeki (1997) was used. The EOS for R-1224yd(Z) is from Akasaka et al. (2017). The EOS for R-1233zd(E) is from Mondéjar et al. (2015). The EOS for R-1336mzz(Z) is from McLinden and Akasaka (2020). The EOS for R-1234yf is from Lemmon and Akasaka (2022).

Table 4
Sensor locations by method.

Method	Sensor types and locations*
1. Evaporator inlet temperature	Pressure sensor for valve inlet flow upstream of the receiver, thermocouple for valve inlet flow 30 cm upstream of the valve. Pressure sensor and thermocouple for outlet flow 1 m downstream of valve.
2. Dew point temperature	Pressure and temperature measurement and sight glass approx. 40 cm downstream of the evaporator (horizontal outlet tube).
3. Density	Coriolis type density meter, installed in liquid line after internal heat exchanger. Pressure sensor upstream of the receiver, thermocouple 1 m downstream of sensor. The temperature measurement was less than 1 K off from built-in temperature sensor of the speed of sound sensor in closer proximity to the density meter.
4. Speed of sound	Installed in liquid line after the internal heat exchanger. Temperature reading from the built-in sensor, pressure sensor upstream of the receiver.
5. Energy balance	Pressure and temperature sensors for refrigerant in proximity up and downstream of the heat exchanger. Water side thermocouples immersed in fluid with tip at the center of the tube.
6. Resting pressure	Pressure averaged over six sensors distributed around the circuit, temperature averaged over 7 sensors distributed around the circuit.

* If not specified otherwise, thermocouples are installed on the outer tube surface and underneath insulation.

Table 5
Measurement uncertainty for used sensors.

Property	Measurement principle	Uncertainty
Temperature	K-type Thermocouples	+/- 1.5 K absolute
High pressure	Piezoelectric	75 kPa absolute
Low pressure	Piezoelectric	15 kPa absolute
Density	Coriolis sensor	10 kg/m^3
Mass flow rate (refrigerant)		<0.5% of reading
Mass flow rate (heat sink)	Coriolis sensor	<0.5% of reading
Sound velocity	Measures time for propagation of wave between geometrically fixed speaker and receiver.	0.01 m/s absolute. An uncertainty of 1 m/s was assumed in the uncertainty calculations for a conservative estimate.

3. Results

3.1. Overview of results

Before attempting to calculate mass fractions from measurements using a solver, it is insightful to study the discrepancies between calculated and measured propeties. Temperature differences are measured by their absolute value while all other differences are measured as a percentage deviation of the measured value:

$$\Delta T = T_{calc} - T_{meas}, \text{ for temperatures}$$

$$\Delta X = \frac{X_{calc} - X_{meas}}{X_{meas}} \cdot 100\%, \text{ for all other}$$

Those deviations were calculated for all data points and all methods. A comprehensive chart showing the results is provided in the appendix (Fig. 6) with additional explanations. Typically deviations were less than 3 K in temperature, 2% in density, 10% for speed of sound and energy balance, and 20% in resting pressure. Deviations found for pure fluids were comparable to those for binary and ternary mixtures. Therefore, we hypothesize that deviations are dominated by systematic measurement uncertainties rather than inaccurate mixture models in REFPROP or errors introduced during charging.

Fig. 5 shows the results of computing the composition based on the six different methods for all binary mixtures. The chart shows the six methods in six columns and all tested binary mixture compositions in 14 rows, resulting in 84 subplots. Each subplot has an x-axis range from 0 to 1; the charged composition is indicated with a black vertical line. The colored dots are the results of the composition determination using the method provided by the column title. The individual dots have different operating conditions. For each subplot, four pieces of information are printed:

- The number of data points displayed (calculations that converged with a mass fraction between 0 and 1.
- The percentage of data points for which the calculation converged.
- The average calculated mass fraction (average of the colored dots in the subplot).
- The deviation of the average calculated to the charged mass fraction. The box is colored in green for deviations of less than 0.025 (2.5

percent by mass), yellow for deviations smaller than 0.055 and orange for deviations greater than that.

Fig. 4 explains how to read the figures with two examples from Fig. 5. Note that dots have the same color as long as their mixtures consist of the same components and vary only by their compositions.

Fig. 5 shows that the Density method has the most green-colored boxes and only two yellow-colored boxes. Hence, this method is superior to the others for the evaluated data by composition determination accuracy. The other methods, usually, have one case with a deviation greater than 0.055 (orange). Still, no deviation is greater than 0.06 except a singular outlier in the energy balance method, and each method has multiple cases with a deviation of less than 0.025 (green). The Energy Balance method's convergence rate is often less than 100%. This is usually due to data points being very close to the vapor dome, for example, with a subcooling at the condenser outlet of less than 0.5 K. When the solver varies the composition; these points can quickly jump across the dome to a different phase such that no satisfying solution is found. This is less likely for the density and speed of sound measurements, which have sensors located far enough downstream from the internal heat exchanger ensuring they are well within the compressed liquid regime.

Table 6 summarizes the results by averaging across different compositions for the three binary mixtures tested. For each method (columns), the respective cell of the table shows the average deviation of the calculated to the charged deviation for all compositions of a binary refrigerant pair. Density shows superior performance with average deviations of 0.01, 0.01 and 0.00 (<0.005) for the pairs R-1234yf /1233zd (E), R-1234yf/1336mzz(Z) and R-32/1224yd(Z). The deviations of all other methods are up to 0.04 or up to 0.03 for the Speed of Sound method. The next section discusses other indicators relevant to choosing a method.

The composition of ternary mixtures could theoretically be calculated using two property measurements. However an investigation of this topic is beyond the scope of this study.

3.2. Comparison of methods

Table 7 compares the six methods plus gas chromatography (GC, not applied in this paper), using the following indicators. The scale is limited to favorable (A/green), intermediate (B/yellow) and disadvantagous (C/red) for simplicity.

- Was the composition determination accurate in this study?
  - Red for the energy balance due to many points without convergence. Great for density. Not applicable for GC.
- How much do the necessary sensors cost?
  - Red for Density, Speed of Sound and GC method, since these devices require investments of more than 5000 USD. Yellow for the Energy Balance method, since it requires flow meters. Green for the other methods which require only temperature and pressure measurements and a sight glass. It should be noted that for large industrial systems with costs of several million USD, the cost of any method would be a small fraction of the total investment cost.
- How strongly does human error impact the results?
  - Only the dew point's visual inspection is susceptible to human bias.
- Can the measurement be collected during normal operation?
  - The dewpoint measurement requires manual operation of the expansion valve but can be done during normal operation (yellow). The resting pressure requires the system to be off and in a thermal equilibrium (C). GC requires refrigerant sampling (B). All other methods can be applied during system operation when ever the system operates at steady-state conditions.

In summary, if a densimeter is affordable, the Density method is the preferred option. If a low cost composition determination is required, the Evaporator Inlet Temperature method is suggested.

Generally, the methods proposed in this study compromise accuracy with convenience and speed of testing. An application-specific decision must be made regarding the utility of any method. A significant advantage of non-invasive online measurements is that the mass fractions can be calculated without taking a sample and during operation. This enables collection of many data points as a byproduct of performance testing or normal operation.

It should also be noted that reference quality equilibrium data is not presently available for any of the mixtures studied here. Presently, the accuracy of these models is therefore in question. However, the close agreement between the thermophysical property data reported in this study and the mixture models suggests they provide reasonable estimates of mixture properties.

4. Conclusions

This study evaluated six non-invasive inline composition determination methods, five of which are online measurements during system operation. The pure fluids R-1233zd(E), R-1336mzz(Z), R-1234yf, R-1224yd(Z), and R-32 were tested along with binary and ternary mixtures thereof. The composition was determined by comparing property predictions from REFPROP v10 with direct measurements for six different properties: saturation temperature after an isenthalpic expansion, dewpoint temperature, subcooled liquid density, subcooled liquid speed of sound, condenser heat transfer rate and resting pressure. Liquid density was the most accurate property for composition determination in this study, with the average deviation for each mixture mostly below 0.01. The evaporator inlet temperature is a much less expensive method and still showed good results with the average deviation being smaller or qual to 0.03 for 10 out of 14 binary mixtures and a maximum average

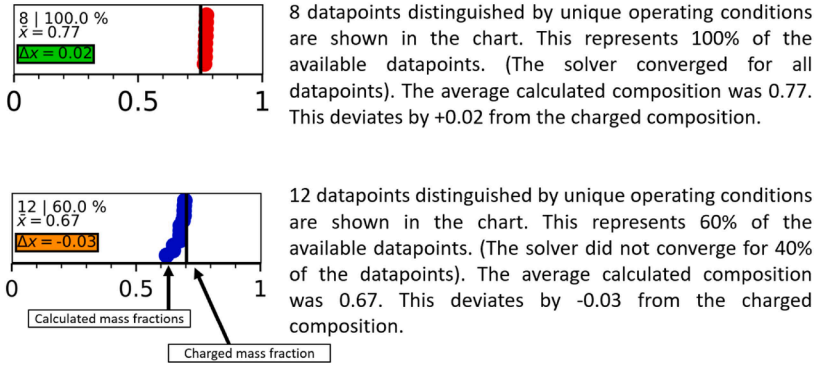

Fig. 4. Explanation of the information in Fig. 5.

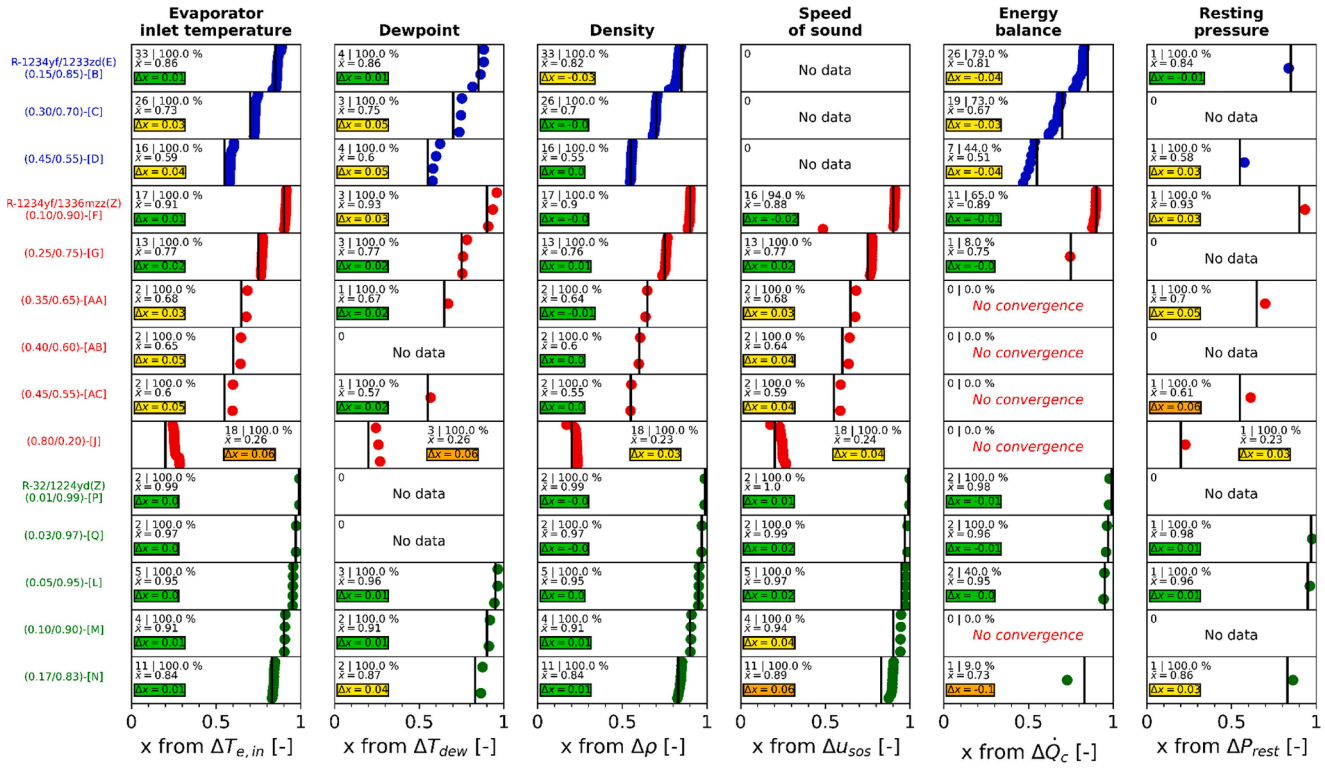

Fig. 5. Mass fractions calculated from measurements. An introduction to the Figure is provided in Fig. 4.

Table 6
Accuracy of composition determination compared to charged mass fraction for each method. The values represent the average deviation for a certain mixture across all the compositions for which data is available.

Binary mixture	Method					
	Evaporator inlet temp.	Dew point temp.	Density	Speed of sound	Energy balance	Resting pressure
R-1234yf /1233zd(E)	0.03	0.04	0.01	no data	0.04	0.02
R-1234yf /1336mzz(Z)	0.04	0.03	0.01	0.03	0.01	0.04
R-32/1224yd(Z)	0.00	0.02	0.00	0.03	0.03	0.02

Table 7
Qualitative comparison of different composition determination methods across different indicators using a three-level scale from favorable (green/A) to disadvantagous (red/C).

Criterion	Method						
	Evap. inlet temperature	Dewpoint temperature	Density	Speed of sound	Energy balance	Resting pressure	Gaschromatography
Performance in this study	B	B	A	B	C	B	N/A
Cost	A	A	C	C	B	A	C
Impact of human error	A	C	A	A	A	A	A
Possible during normal operation	A	B	A	A	A	C	B

deviation of 0.06. For the majority of 380 datapoints across 14 binary mixtures, the mass fraction was predicted with a deviation of no more than 0.05 by all methods. The Energy Balance method was most prone to convergence issues. Based on the good agreement of measurements and property predictions using REFPROP v10, the tested mixture models are judged accurate enough for the system-level design of refrigeration plants. This was true both for binary and ternary mixtures. Additionally, the data from this study can be used to motivate the development of new

reference quality mixture models for the studied refrigerants and enable more reliable mixture determinations. Property data of ternary mixtures was also found to be in good agreement with REFPROP predictions, but a composition determination was not attempted. This paper is a step towards robust online composition determination in heat pumps with high-glide mixtures.

Nomenclature

Symbol	Meaning	Unit
DP	Dewpoint temperature	°C
h	Enthalpy	kJ/kg
IHX	Internal heat exchanger	
m	Charge (mass of refrigerant)	
$\dot{m}$	Mass flow rate	kg/min
P	Pressure	kPa
$\dot{Q}$	Heat transfer rate	kW
q	Vapor quality (1 is saturated steam, 0 is a saturated liquid)	
ρ	Density	kg/m^3
RP	Resting pressure	kPa
u	Speed of sound	m/s
V	Volume	Liter
x	Mass fraction	–
Subscripts	**Meaning**	
1, 2, 3	Mixture component 1, 2 or 3	
calc	Calculated	
c	Condenser	
dew	At dewpoint pressure	
e	Evaporator	
equ	Equilibrium	
hp	Heat pump	
in	Inlet	
meas	Measured	
out	Outlet	
r	Refrigerant	
si	Heat sink	
v	Valve	
W	Water	

CRediT authorship contribution statement

Leon P.M. Brendel: Conceptualization, Writing – original draft. **Silvan N. Bernal:** Investigation. **Carl Hemprich:** Investigation, Writing – review & editing. **Aaron J. Rowane:** Writing – review & editing. **Ian H. Bell:** Writing – review & editing. **Dennis Roskosch:** Conceptualization, Writing – review & editing. **Cordin Arpagaus:** Conceptualization, Writing – review & editing. **André Bardow:** Conceptualization, Funding acquisition. **Stefan S. Bertsch:** Conceptualization, Funding acquisition.

Declaration of competing interest

The authors declare that they have no known competing financial interests or personal relationships that could have appeared to influence the work reported in this paper.

Acknowledgments

The help of several colleagues in building the HTHP is gratefully acknowledged and was essential in producing the presented results. In addition, the authors gratefully acknowledge the financial support of the Swiss National Science Foundation and Innosuisse (Bridge Discovery project with grant number 203645).

The authors also gratefully acknowledge the financial support of the Swiss Federal Office of Energy SFOE as part of the SWEET (Swiss Energy Research for the Energy Transition) project DeCarbCH (DeCarbonisation of Cooling and Heating in Switzerland, www.sweet-decarb.ch). The contents and conclusions of this research are the authors' sole responsibility.

The internal NIST funding for collaboration is gratefully acknowledged.

Appendix

Procedures embedded in methods

Table 8
Functional form of composition determination methods.

Name and functional form	Primary path to reference property Obtaining property without using REFPROP	Secondary path to reference property Obtaining property using REFPROP
Evaporator inlet temperature ($T_{v,out}$) $x_1 = f(P_{v,out}, T_{v,out}, P_{v,in}, T_{v,in})$ *Note: Assume isenthalpic expansion*	Direct measurement of $T_{v,out}$	$h_{v,in} = f_{REF}(P_{v,in}, T_{v,in})$ $T_{v,out} = f_{REF}(P_{v,out}, h_{v,in})$
Dewpoint temperature (T_{dew}) $x_1 = f(P_{e,out}, T_{dew}, q = 1)$	Direct measurement of T_{dew}	$T_{dew} = f_{REF}(P_{e,out}, q = 1)$
Density ($\rho_{v,in}$) $x_1 = f(P_{v,in}, T_{v,in}, \rho_{v,in})$	Direct measurement of $\rho_{v,in}$	$\rho_{v,in} = f_{REF}(P_{v,in}, T_{v,in})$
Speed of sound ($u_{v,in}$) $x_1 = f(P_{v,in}, T_{v,in}, u_{v,in})$	Direct measurement of $u_{v,in}$	$u_{v,in} = f_{REF}(P_{v,in}, T_{v,in})$
Condenser heat transfer rate ($\dot{Q}_c$) $x_1 = f(P_{c,in}, T_{c,in}, P_{c,out}, T_{c,out}, \dot{m}_r, T_{si,in}, T_{si,out}, \dot{m}_{si})$ *Note: Assume energy balance closed*	$h_{si,out} = f_{REF}(P_{si,out}, T_{si,in})$ $h_{si,in} = f_{REF}(P_{si,in}, T_{si,in})$ $\dot{Q}_c = \dot{m}_{si}(h_{si,out} - h_{si,in})$	$h_{c,in} = f_{REF}(P_{c,in}, T_{c,in})$ $h_{c,out} = f_{REF}(P_{c,out}, T_{c,in})$ $\dot{Q}_C = \dot{m}(h_{c,in} - h_{c,out})$
Resting pressure (P_{equ}) $x_1 = (T_{equ}, P_{equ}, V_{hp}, m_r)$	Direct measurement	$\rho_{tot} = Charge/V_{hp}$ $P_{equ} = f_{REF}(T_{equ}, \rho_{tot})$

Deviations of measured and calculated data

Structure of chart and overall observations

Fig. 6 shows deviations of measured and calculated values. The figure shows six columns for the six different methods of composition determination and thirty rows, one row per mixture composition shown in Table 2, resulting in 180 subplots. For example, the top left subplot shows all steady-state data points collected for pure R-1233zd(E), and each data point is a deviation of the measured and calculated evaporator inlet temperature at a certain operating condition. The mixtures of each row are printed in the very left column with its associated letter.

The data points per subplot are sorted from top to bottom with a decreasing absolute deviation. The scale is shown below the 30th row of subplots. There are 2 values printed in the top left corner of each subplot. The first is the number of data points shown in the subplot. The second is the percentage of data points from the series shown in the chart. Hence, the text "20 | 95%" means that 20 data points are displayed and that those 20 data points are 95% of the data points available for this series and method. Therefore, 5% of the data points for this series and method are outside the x-axis scale range.

It should be noted that the x-axis scales are different for the varying methods.

The first five rows are dedicated to pure fluids. Hence, those deviations are not impacted by mixture properties but due to the measurement and charging procedures, heat losses or sensor uncertainties. A mixture showing stronger deviations could indicate fractionation or an inaccurate property model. However, only very few mixture datasets, if any per method, show a greater deviation than the deviation known from the pure fluids.

The density measurements stand out because almost all data points showed a deviation of less ±3% between the measured and calculated values. There is also no systematic trend towards negative or positive deviations.

Detailed observations

Evaporator inlet temperature. Typically, the deviations are within −3 to 0 K, where a negative value means the calculated temperature is smaller than the measured temperature. R-1234yf (H-series) has a deviation of at least 1.5 K, while the other pure fluids deviate consistently less. The AB, AC, AD and AE series all show deviation of at least −3 K. Since these mixtures were created consecutively without recovering the entire charge, the deviations could be caused by a contamination introduced in the AB series, which then effects all successive series until a complete evacuation of the system (a complete evacuation can be identified whenever the total charge reduces while the (chronological) letters increase).

Dew point temperature. The pure fluids' dew point temperature measurements aligned with the calculations well, except for R-1234yf (H-series). Two dew point measurements were conducted for R-1234yf. One had a deviation of −2.5 K and the other of −5.5, falling out of the range of the chart (note the "50%" printed in the top left corner, indicating that only 50% of the data falls within the range of the x-axis.

Density. All density measurements and calculations deviated less than ±3%, for most data points the deviation was even smaller than ±2%, making the method very promising for composition determination.

Speed of sound. The x-axis scale has a range of ±15%, three times larger than the density scale. The deviations are smaller than approximately ±5% for pure fluids and all the R-1234yf/1336mzz(Z) mixtures (red). However, all mixtures containing R-32 show a systematically increased deviation that cannot be readily explained, especially since the density measurements directly upstream of the speed of sound measurements do not show great deviations. Inaccurate property models for the pure fluids is a potential reason.

Condenser energy balance. The deviation is within −10 to 0% for most of the data points. Negative deviations are expected due to the heat losses from the condenser, which operated between 70 and 120 °C for most datapoints. Overall, the pure fluids and mixtures show similar deviations, suggesting that they result from systematic measurement errors and not from an inaccurate property model.

Resting pressure. The resting pressures of pure fluids deviates consistently by about 5% from the expected values. A positive deviation means the calculated pressure is larger than the measured one. A possible reason is the effect of lubricant in the system. For the mixtures, the deviations typically increase to 5 to 20%, with some outliers to higher and lower deviations. The reason for the larger deviations is unclear. It is important to note that this method utilizes the density known from the inner volume and the total mass of the charged refrigerant. Hence, if a leakage had occurred, it would impact the results.

Sensitivity of properties to changes in mass fraction

Comparing the sensitivity of a property as a function of the mass fraction is also insightful. For example: How much does the dew point temperature at a given pressure change as the composition is changed by 0.01? This gradient was calculated for all data points and the results are shown in Fig. 7. The two numbers in the top left corner of each subplot provide two information: The number of data points plotted in the subplot and the percentage of datapoints displayed relative to the total number the available data points. Hence, if the second number is not 100%, some data points resulted in slopes greater than the axis limits. Generally, where the gradients are strong, a composition determination is easier. Where the gradients are small, the property sensor must have a relatively higher accuracy.

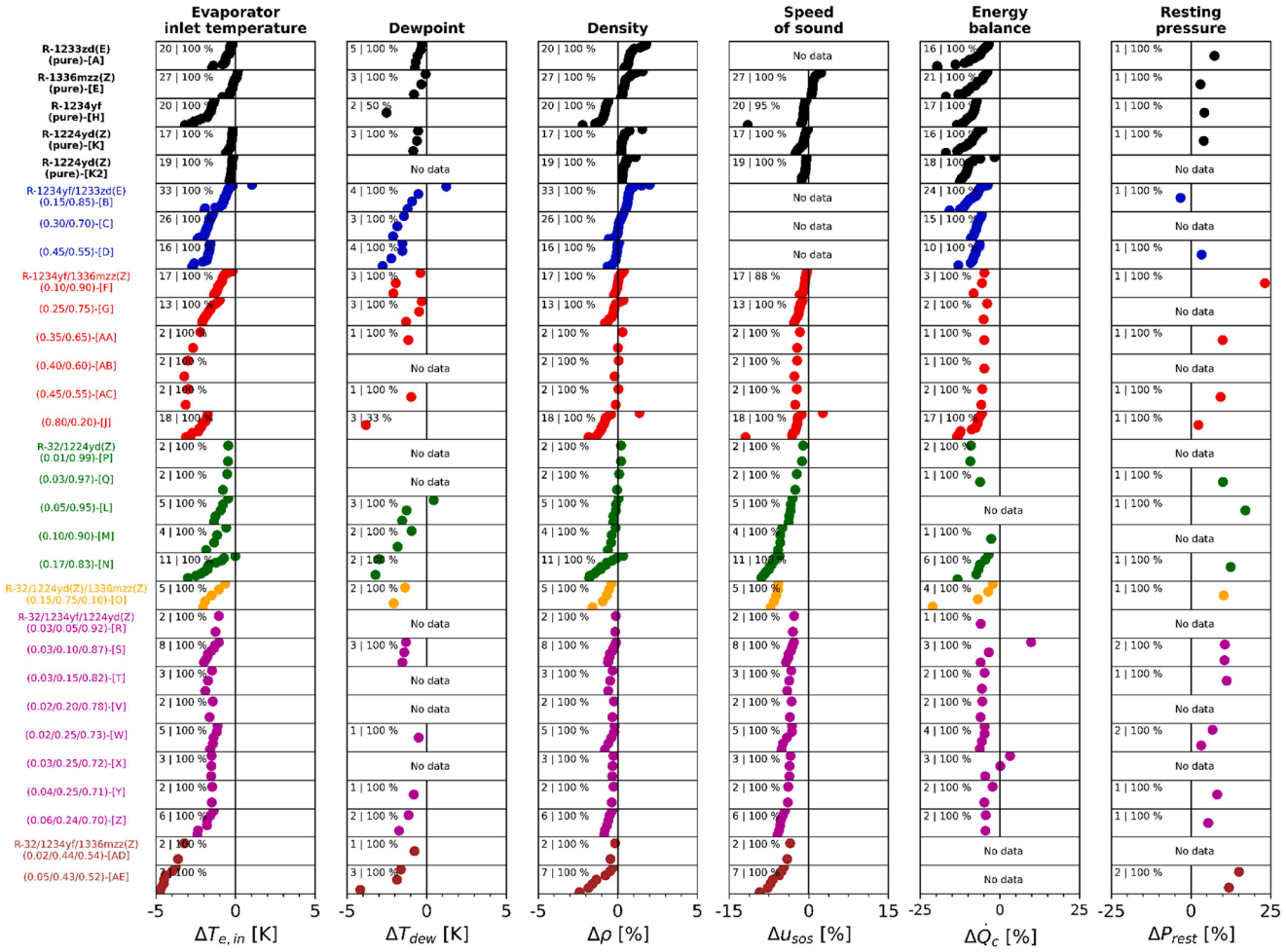

Fig. 6. Deviation of measurements and results expected from calculations using mixture property predictions from REFPROP.

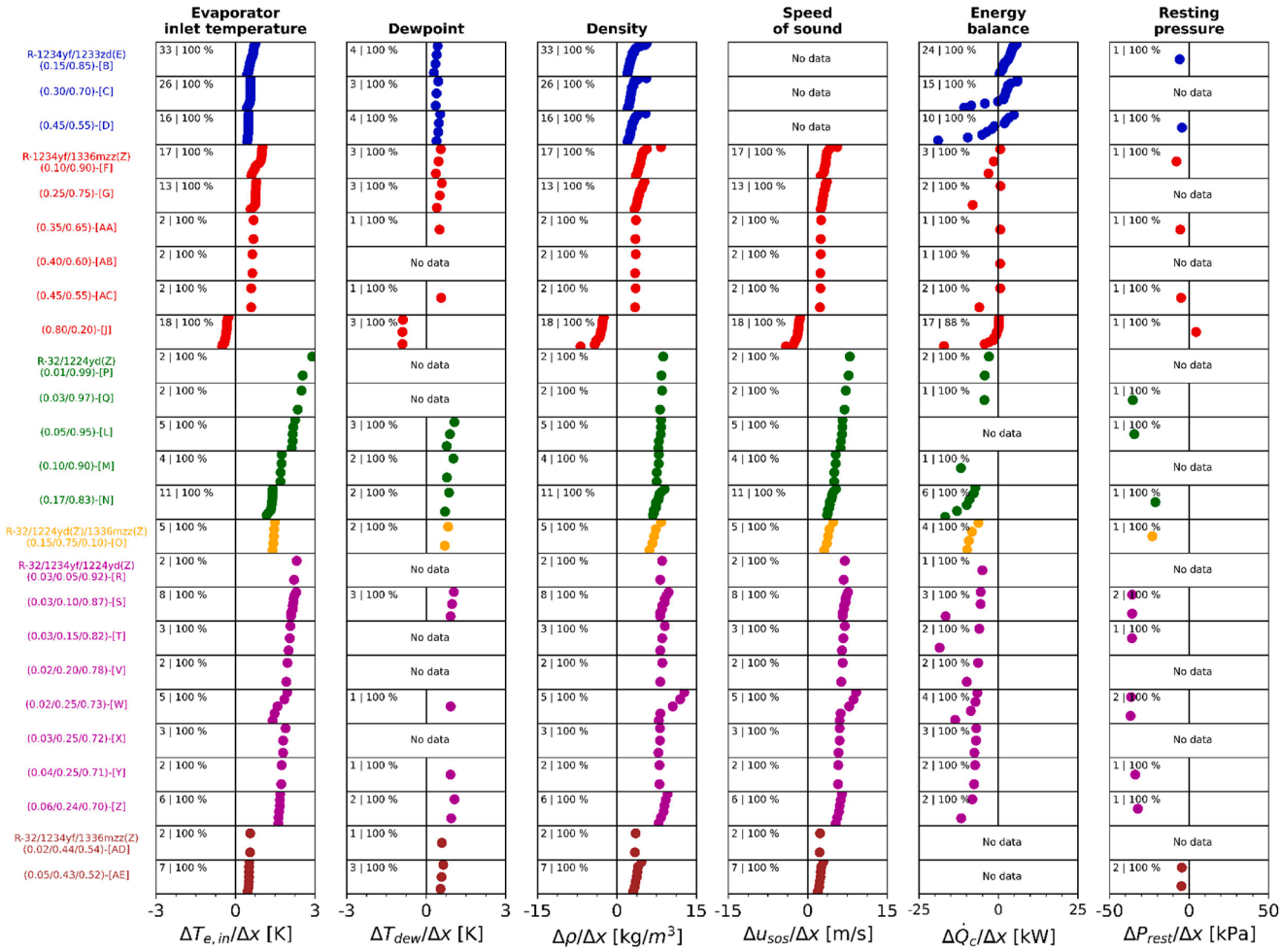

Fig. 7. Property sensitivity to a change of 0.01 in the mass fraction.

References

Abbadi, J.E., Coquelet, C., Valtz, A., Houriez, C., 2022. Experimental measurements and modelling of vapour−liquid equilibria for four mixtures of 2,3,3,3−tetrafluoropropene (R1234yf) with 1,1,1,2−tetrafluoroethane (R134a) or 1,1−difluoroethane (R152a) or trans−1−chloro−3,3,3−trifluoropropene (R1233zd (E)) or 2−chloro−3,3,3−trifluoropropene (R1233xf). Int. J. Refrig. 140, 172–185. https://doi.org/10.1016/j.ijrefrig.2022.05.006.

Akasaka, R., 2013. Thermodynamic property models for the difluoromethane (R-32)+ trans-1,3,3,3-tetrafluoropropene (R-1234ze(E)) and difluoromethane+2,3,3,3-tetrafluoropropene (R-1234yf) mixtures. Fluid. Phase Equilib. 358, 98–104. https://doi.org/10.1016/j.fluid.2013.07.057.

Akasaka, R., Fukushima, M., Lemmon, E.W., 2017. A Helmholtz Energy Equation of State for cis-1-chloro-2,3,3,3-Tetrafluoropropene (R-1224yd(Z)). In: Presented at the European Conference on Thermophysical Properties. Graz, Austria.

Aprea, C., de Rossi, F., Renno, C., 2009. Analysis of some recharge solutions on varying the R407C composition. Energy Convers. Manag. 50, 2288–2295. https://doi.org/10.1016/j.enconman.2009.05.005.

Bao, J., Zhao, L., 2016. Experimental research on the influence of system parameters on the composition shift for zeotropic mixture (isobutane/pentane) in a system occurring phase change. Energy Convers. Manag. 113, 1–15. https://doi.org/10.1016/j.enconman.2016.01.017.

Bell, I.H., 2023. Mixture Model for Refrigerant Pairs R-32/1234yf, R-32/1234ze(E), R-1234ze(E)/227ea, R-1234yf/152a, and R-125/1234yf. J. Phys. Chem. Ref. Data 52, 013101. https://doi.org/10.1063/5.0135368.

Bell, I.H., Riccardi, D., Bazyleva, A., McLinden, M.O., 2021. Survey of Data and Models for Refrigerant Mixtures Containing Halogenated Olefins. J. Chem. Eng. Data 66, 2335–2354. https://doi.org/10.1021/acs.jced.1c00192.

Brendel, L.P.M., Bernal, S.N., Arpagaus, C., Roskosch, D., Bardow, A., Bertsch, S.S., 2023. Experimental investigation of high-glide refrigerant mixture R1233zd(E)/R1234yf in a high-temperature heat pump. In: Presented at the International Congress of Refrigeration. Paris, France.

Brendel, L.P.M., Bernal, S.N., Widmaier, P., Roskosch, D., Bardow, A., Bertsch, S.S., 2024. High-Glide Refrigerant Blends in High-Temperature Heat Pumps: part 1 – Coefficient of Performance. Int. J. Refrig. Publication in progress.

Chen, J., Kruse, H., 1995. Calculating Circulation Concentration of Zeotropic Refrigerant Mixtures. HVACR Res. 1, 219–231. https://doi.org/10.1080/10789669.1995.10391320.

Chen, Q., Yan, G., Yu, J., 2021. Experimental research on the concentration distribution characteristics of dual-temperature refrigeration system using R290/R600a based on separation condensation. Int. J. Refrig. 131, 244–253. https://doi.org/10.1016/j.ijrefrig.2021.06.024.

Fuchs, 2023. Reniso Triton SE170 [WWW Document]. Fuchs Lubr. Ger. GmbH. URL. https://www.fuchs.com/de/en/product/product/148791-RENISO-TRITON-SE-170/.

Fuchs, 2022. Reniso Triton SE 170 - Synthetic refrigeration oil based on polyol esters (POE) for HFC/FC and HFO refrigerants - including HFO/HFC refrigerant blends.

Fukuda, S., Takata, N., Koyama, S., 2012. The Circulation Composition Characteristic of the Zeotropic Mixture R1234ze(E)/R32 in a Heat Pump Cycle. In: Presented at the Purdue Conferences. West Lafayette, IN, USA.

Fukuta, M., Yanagisawa, T., Shimasaki, M., Ogi, Y., 2006. Real-time measurement of mixing ratio of refrigerant/refrigeration oil mixture. Int. J. Refrig. 29, 1058–1065. https://doi.org/10.1016/j.ijrefrig.2006.03.010.

Johansson, A., Lundqvist, P., 2001. A method to estimate the circulated composition in refrigeration and heat pump systems using zeotropic refrigerant mixtures. Int. J. Refrig. 24, 798–808. https://doi.org/10.1016/S0140-7007(00)00061-X.

Lemmon, E.W., Akasaka, R., 2022. An International Standard Formulation for 2,3,3,3-Tetrafluoroprop-1-ene (R1234yf) Covering Temperatures from the Triple Point Temperature to 410 K and Pressures Up to 100 MPa. Int. J. Thermophys. 43, 119. https://doi.org/10.1007/s10765-022-03015-y.

Lemmon, E.W., Bell, I.H., Huber, M.L., McLinden, M.O., 2018. NIST Standard Reference Database 23: Reference Fluid Thermodynamic and Transport Properties-REFPROP, Version 10.0. National Institute of Standards and Technology. https://doi.org/10.18434/T4/1502528.

McLinden, M.O., Akasaka, R., 2020. Thermodynamic Properties of *cis* -1,1,1,4,4,4-Hexafluorobutene [R-1336mzz(Z)]: vapor Pressure, (*p*, ρ, *T*) Behavior, and Speed of

Sound Measurements and Equation of State. J. Chem. Eng. Data 65, 4201–4214. https://doi.org/10.1021/acs.jced.9b01198.

Miyawaki, K., Ikeda, S., Hiratsuka, K., Shikazono, N., 2023. Situ Measurement of Circulation Composition of Refrigerant Mixture in Heat Pump System with NIR Absorption Spectroscopy. Int. J. Refrig. S0140700723000336. https://doi.org/10.1016/j.ijrefrig.2023.01.023.

Mondéjar, M.E., McLinden, M.O., Lemmon, E.W., 2015. Thermodynamic Properties of trans-1-Chloro-3,3,3-trifluoropropene (R1233zd(E)): vapor Pressure, (p, ρ, T) Behavior, and Speed of Sound Measurements, and Equation of State. J. Chem. Eng. Data 60, 2477–2489. https://doi.org/10.1021/acs.jced.5b00348.

Quenel, J., Anders, M., Atakan, B., 2023. Propane-isobutane mixtures in heat pumps with higher temperature lift: an experimental investigation. Therm. Sci. Eng. Prog. 42, 101907 https://doi.org/10.1016/j.tsep.2023.101907.

Sumida, Y., Okazaki, T., Kasai, T., Ueno, Y., 1998. Development of the Circulating Composition Sensing Circuit for a Multiple Split Type Air Conditioner with R-407C. In: Presented at the Purdue Conferences. West Lafayette, IN, USA.

Tillner-Roth, R., Yokozeki, A., 1997. An International Standard Equation of State for Difluoromethane (R-32) for Temperatures from the Triple Point at 136.34 K to 435 K and Pressures up to 70 MPa. J. Phys. Chem. Ref. Data 26, 1273–1328. https://doi.org/10.1063/1.556002.

Virtanen, P., Gommers, R., Oliphant, T.E., Haberland, M., Reddy, T., Cournapeau, D., Burovski, E., Peterson, P., Weckesser, W., Bright, J., van der Walt, S.J., Brett, M., Wilson, J., Millman, K.J., Mayorov, N., Nelson, A.R.J., Jones, E., Kern, R., Larson, E., Carey, C.J., Polat, İ., Feng, Y., Moore, E.W., VanderPlas, J., Laxalde, D., Perktold, J., Cimrman, R., Henriksen, I., Quintero, E.A., Harris, C.R., Archibald, A.M., Ribeiro, A. H., Pedregosa, F., van Mulbregt, P., SciPy 1.0 Contributors, 2020. SciPy 1.0: fundamental Algorithms for Scientific Computing in Python. Nat. Methods 17, 261–272. https://doi.org/10.1038/s41592-019-0686-2.

Zhang, J., Elmegaard, B., Haglind, F., 2021. Condensation heat transfer and pressure drop characteristics of zeotropic mixtures of R134a/R245fa in plate heat exchangers. Int. J. Heat Mass Transf. 164, 120577 https://doi.org/10.1016/j.ijheatmasstransfer.2020.120577.